Research paper

Research on energetic characteristics of explosive containing B/Al

Qingguan Song*, Wei Cao*, Dayuan Gao*[†], Xinglong Li*,
Baohui Zheng*, and Xiangli Guo*

*Institute of Chemical Materials, China Academy of Engineering Physics, Mianyang, Sichuan 621999, CHINA
  Phone: +86−816−2485366

[†]Corresponding author: gaodayuan@caep.cn

Abstract

Novel HMX (octahydro-1.3,5,7-tetranitro-1,3,5,7-tetrazonicine) based metalized explosive formulations, containing boron and aluminum (B/Al) powders, hydroxyl-terminated polybutadiene (HTPB) and belonging to the enhanced blast explosive, were designed and prepared. Investigations of the energetic characteristics of the new metalized explosives were undertaken to improve such composite explosive formulations. The impact sensitivity and friction sensitivity were measured which made a full acknowledgement of the safety of metalized explosive under different external energy stimuli. The detonation velocity and detonation pressure were measured using spring electric pin method and plate dent test, respectively. The explosion heat was measured in a calorimetric bomb filled with nitrogen (N_2) and the cylinder expansion test was performed. From the cylinder test data the wall velocity and the Gurney energy of the explosives were determined. Then, the isentrope exponents of the composite detonation products were estimated numerically with hydrodynamic code. Finally, the JWL equation of state of the detonation products was determined for each explosive according to our test data. The effect of the Al and B content on the detonation characteristics is also checked.

1. Introduction

Explosives with metal additives named metallized explosives have played a large role in the defense industry due to their higher energy output than current non-metal explosives[1]. As a metal additive, boron (B) has extremely high gravimetric and volumetric heating values when compared with aluminum (Al), magnesium (Mg), beryllium (Be), lithium (Li), silicon (Si) and other energetic metals[2]. In addition, some of these metal additives have drawbacks that limit their application[3]. Currently, Al as a metal additive is commonly added to explosives and propellants in order to generate higher energy release and longer pressure pulses[4]−[6].

Many papers have been published on the effects of B used in propellants[7]−[9]. It is proved that the B powder can improve the heat of combustion in propellants. However, the ignition of B particle takes a long time because of the high ignition temperature of B[10]. In addition, the B_2O_3 in the product gas coats has been proven unreacted B and causes a low combustion efficiency. Furthermore, the melting and burning temperature of B_2O_3 are 450 ℃ and 2065 ℃[11], respectively, causing further combustion efficiency loss with increasing B content.

To overcome these drawbacks of B in explosives, combining less ignitable metals with other more ignitable metals in metallized explosives provides a solution to enhancing the explosion energy of these explosives and gaining the highest energy output possible[12]. Considering that the high burning temperature of Al is close to 2200 ℃[13], the combination of Al and B is one such energetic system that shows great promise. The Al and B materials can be mechanically mixed to create an energetic composite capable of being designed for necessary applications, then the longer duration and high temperatures generated by the B/Al composite after explosion can be utilized. Although B has seen some investigations as an additive for better explosion performance[14]−[16], B/Al composite powder has rarely been investigated. Mixtures of B/Al composite and explosive were studied by Lee et al.[17], who found that the

quasi-static pressure of the formulation containing B/Al composite in a confined chamber performed 1.3 times better as compared to the formulation containing pure Al. Xu et al.[18),19)] studied the combustion heat of the B/Al composite powders and its application in metallized explosives in underwater explosions, indicating that the addition of B/Al composite powders to explosives was a good way to enhance their blast effect, to improve the temperature of the explosion field and to prolong the duration of the higher temperature.

These new metallized explosives show potential high energy and high blast performance equal or greater than current combined effects explosives. However, there still remains a lack of information concerning the reaction mechanism of the various detonation products with B/Al composite powders under different environments. The objective of this research was to investigate, in a controlled environment, the explosive parameter enhancement effects of various forms of metallized explosives containing B/Al and to compare their relative performance against the pure aluminized explosive.

2. Experimental
2.1 Sample preparation of the metalized explosives

The investigated metalized explosives shown in Figure 1 are prepared by melting and kneading method, and the metal molds of $\Phi 100 \times 105$ mm are charged with vacuum vibration instrument. The explosive molds are opened after curing about 240 hours at 50℃, and then the explosive cylinders are cooled to room temperature.

The metalized explosives contain a number of crystals of HMX as a high explosive ingredient, Al and B as metallic fuels, and the whole is consolidated by HTPB as a binder. Names and composition of the composite granules are given in Table 1. The desensitized HMX with particle size 6.7 μm is coated by wax with content of 2 wt% Al powder with particle sizes 1–5 μm and B powder with particle sizes 1–5 μm are used. The average molecular weight of HTPB is 2000 g·mol^{-1}.

The micro morphology of Al powder, B powder and B/Al compound powders are observed by scanning electron microscope (SEM), and the SEM images at various scales are obtained in Figure 2. Al powders are spherical particles, and partial particles have agglomeration. The structure of B powders is amorphous flake crystallite shape whose sizes are between 1–5 μm. For the B/Al compound powders, there are many small amorphous flake B powders on the surface of Al powders.

2.2 Impact sensitivity measurement

According to the GJB 772A-97 601.1 impact sensitivity explosive probability method[20)], impact sensitivity is measured by the drop-weight impact sensitivity test (DWIST). The DWIST equipment consists of the electric control units, drop hammer of 2 kg weight, and tested sample of 50 mg. Impact sensitivity is expressed by explosion probability (I) among 25 different impact tests. The greater I, the higher the impact sensitivity.
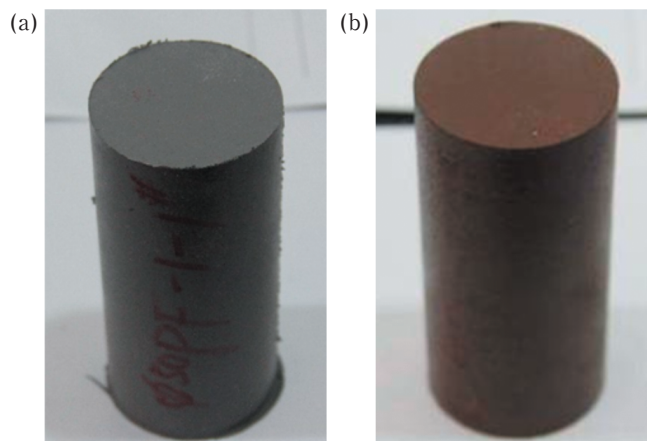

Figure 1   Samples of metalized explosive cylinders containing (a) Al and (b) B/Al.

Table 1   Formulations of explosives containing B and Al.

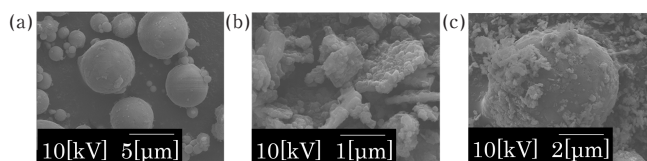| Sample	Composition [wt%]			
	HMX	B	Al	HTPB
GH-1	60	8	12	20
GH-2	60	4	16	20
GH-3	64	7.2	16.8	12
GH-4	64	6.6	15.4	14
GH-5	64	4	16	16
PF-1	64	–	20	16
PF-2	64	6	14	16
PF-3	64	10	10	16

Figure 2   SEM paragraphs of (a) Al powders, (b) B powders and (c) B/Al powders.

2.3 Friction sensitivity measurement

Friction sensitivity is tested by MGY-1 pendulum friction apparatus which is built with GJB 772A-97 601.2 friction sensitivity explosive probability method[20)]. The testing condition of MGY-1 are sample of 30 mg and pendulum of 1.5 kg and 90° angle. Friction sensitivity is expressed by explosion probability (F) among 25 different friction tests. The greater F, the higher the friction sensitivity.

2.4 Spring electric pin method and plate dent test

In the spring electric pin method and plate dent test, the representative device is shown in Figure 3, in which the metalized explosive cylinders of $\Phi 50 \times 220$ mm are samples to be tested and the HMX based cylinders of $\Phi 50 \times 50$ mm are booster explosives. The initiating system consists of PETN tablet and industrial detonator.

The detonation velocities are measured with 7 spring electric pins of $\Phi 0.7$ mm attached to the cylinder surface. The reaching times of detonation wave are recorded with the pins according to the electric conductivity of detonation products. Then, the detonation velocity can be

calculated by the distance and time difference between two pins.

The plate dent test is one of the most useful tools to determine the detonation pressure. In the plate dent test, the witness plate is Q_{235} steel cylinder of $\Phi 100 \times 40$ mm. After detonation of explosives, the depth of dent produced in witness plate can be measured by a depth micrometer. Then, with the given empirical relationship between detonation pressure and dent depth[21], the detonation pressure of this new metalized explosive can be relatively evaluated.

2.5 Calorimetric heat of explosion measurements

The calorimetric heat of explosion of the tested composites is determined according to the method described in literature[22]. The heat is measured using a 5 L calorimetric bomb filled with N_2 under an absolute pressure of 1.2 MPa. Samples of the explosives (about 25 g) are pressed into 30 mm long cylindrical pellets with a diameter of 25 mm.
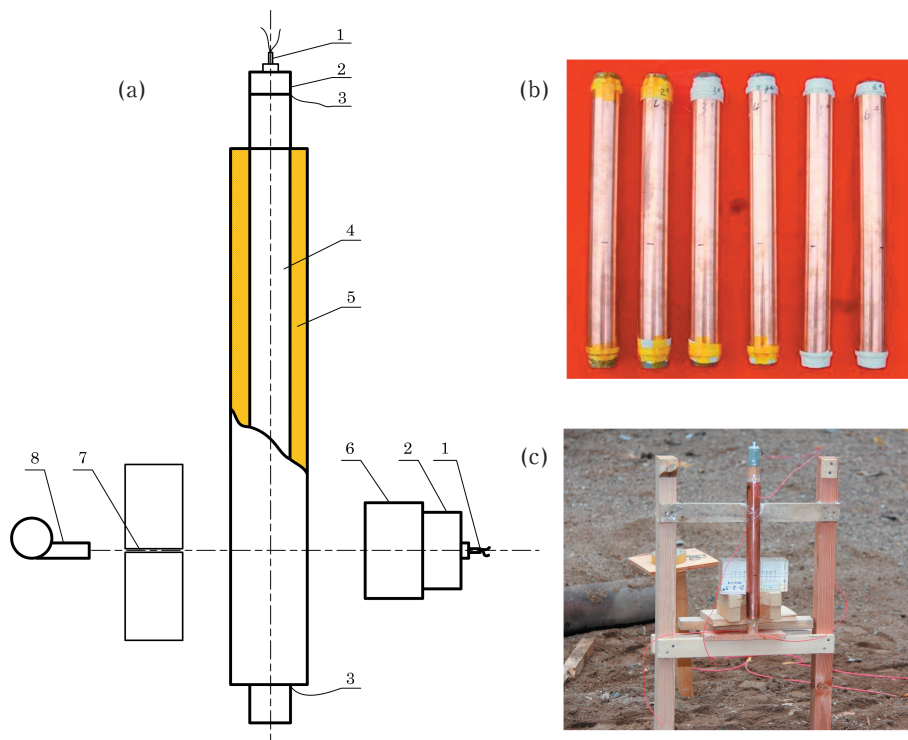
2.6 Cylinder test

The cylinder test results are the basis for the determination of the acceleration ability and energetic characteristics.

For the metalized explosives PF-1, PF-2 and PF-3, each investigated composite explosive is pressed into ten 50 mm long cylindrical charges with a diameter of 50 mm. Then, these charges are inserted into 500 mm long and 60.2 mm external diameter copper tube, seen in Figure 4. The densities are 1.708, 1.689 and 1.673 g·cm^{-3} for the explosives PF-1, PF-2 and PF-3, respectively. The cylinder test system are composed of high voltage electric detonator, booster explosive, copper cylinder filled with metalized explosive, electric probe, background light source, metal plate with slit and high speed scanning camera. The 50 mm cylinder is placed parallel to the ground. The background light source of the cylinder is the explosive luminescence of argon bomb. The high speed scanning camera records the expansion distance of the cylinder in the stable detonation section of the explosive through the slit of the metal plate. The scanning speed of the high-speed scanning camera is 3.0 mm·μs^{-1}. The
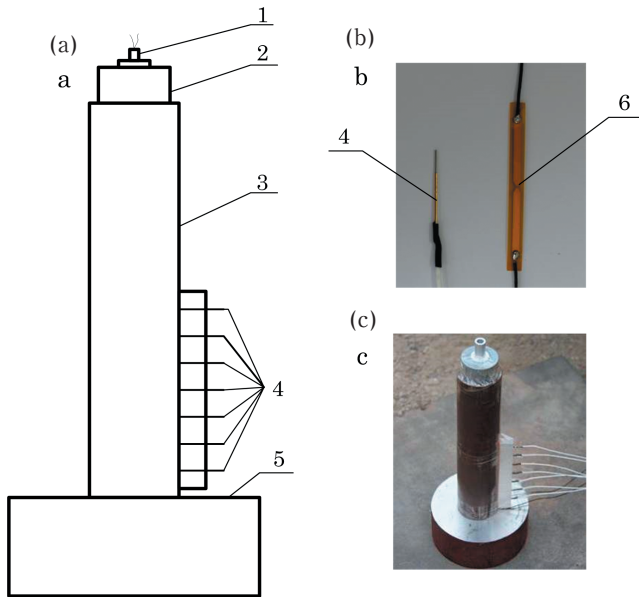
Figure 3   Schematic diagram of spring electric pin method and plate dent test. (a) schematic diagram 1-detonator, 2-booster explosive, 3-metalized explosive, 4-spring electrical pin, 5-steel witness plate, 6-copper foil pin (b) electric pins (c) site layout.

Figure 4   Experimental setup of 50 mm cylinder test. (a) schematic diagram 1-detonator, 2-booster, 3-electric pin, 4-metalized explosive, 5-cooper cylinder, 6-argon lighting source, 7-slit, 8- high speed camera (b) charge with cooper cylinder (c) site layout.

detonation velocity of the explosive is measured with an ionization probe. The distance between the two electric probes is 533.3 mm.

3. Results and discussion
3.1 Mechanical sensitivities

The safety of explosive containing B/Al was evaluated by sensitivity test, and the safety risk assessment for preparation and processing of kilogram grade sample was also evaluated. Several kinds of HMX based explosives containing B/Al were designed and prepared. According to the impact and friction sensitivity explosive probability methods, the mechanical sensitivity of explosives containing B/Al were measured. The test results of mechanical sensitivities are shown in Table 2, where the impact sensitivity and friction sensitivity are expressed by symbols I and F, respectively.

As shown in Figure 2, Al powders are spherical shape while the B powders are amorphous flake crystallite shape. For B/Al compound powders, since there are many irregular parts on the surface of Al powders, the stress concentration in B/Al compound powder can easily be formed under action of external mechanical energy. The hot-spots can be formed and the explosive can be ignited, so that the impact and friction sensitivity are increased obviously. From Table 2, the mechanical sensitivity of formulations GH-1, GH-2, PF-1, PF-2 and PF-3 are less than 40%, therefore the safety requirement for the preparation and processing technology of mixed explosive is satisfied. In order to obtain high-energy metalized explosives, PF-1, PF-2 and PF-3 which have more explosive ingredients are identified to investigate their detonation characteristics.

Table 2   Mechanical sensitivities of explosives containing B and Al.

Sample	I [%]	F [%]
GH-1	8	24
GH-2	0	20
GH-3	48	36
GH-4	20	56
GH-5	4	84
PF-1	4	10
PF-2	12	20
PF-3	24	32

3.2 Detonation velocity and pressure

The experimental detonation velocities of the explosives PF-1, PF-2 and PF-3 were measured using spring electric pin method and plate dent test. Table 3 summarizes the obtained experimental results.

The difference between explosive PF-1, PF-2 and PF-3 is the contents of B powder and Al powder, while the total content of metal powder is 20%. The density of explosive formula PF-1 and PF-2 is 1.693 g·cm^{-3}, and the density of explosive formula PF-3 is 1.694 g·cm^{-3}, which indicate that explosive with high quality uniformity, can be obtained by void vibration. The detonation velocity of PF-1 is 7.833 mm·µs^{-1}. By adding 6% and 10% B into explosives, the detonation velocities increase slightly by 1.6% and 2.4% respectively. The large content of B powders means the larger detonation velocity. It is inferred that the combination effect of B/Al compound powders makes a small part of the compound powders take reaction in detonation reaction region, which leads to increasing detonation velocity. However, comparison between the detonation pressures from Table 3 suggests that there is no obvious change by adding 6% and 10% B into explosives. Therefore, in general, it is understood that B/Al compound powders are chemically inert in the detonation reaction zone of high explosives and they burn during the expansion of detonation products. Their reaction kinetics are not fast enough to react with the detonation products in that zone and they behave like inert.

3.3 Calorimetric heat of explosion

Two measurements were performed for each explosive. The obtained results are presented in Table 4.

The calorimetric heats of the explosives are considerably higher than that determined for pure HMX (5.5850 kJ·g^{-1}) [23]. This means that a significant part of Al and B powder takes part in the reactions with gaseous detonation products and additional energy is released during their expansion in later time. Considering that the combustion heat of B is almost two times than that of Al, the calorimetric heats of PF-2 (6.5657 J·g^{-1}) and PF-3 (6.1849 J·g^{-1}) are higher than that of PF-1 (5.8387 J·g^{-1}) only containing Al. This means that both Al and B powder all react in the process of explosion. However, the calorimetric heat of PF-3 containing more content of B is

Table 3   Detonation velocity and pressure of explosives containing B/Al.

Sample	ρ [g·cm^{-3}]	D [mm·µs^{-1}]	P [GPa]	γ
PF-1	1.693±0.003	7.833±0.032	23.69±0.11	3.38±0.06
PF-2	1.693±0.003	7.959±0.045	23.61±0.16	3.54±0.09
PF-3	1.694±0.003	8.018±0.068	23.89±0.19	3.61±0.17

Table 4   Calorimetric explosion heats of explosives containing B and Al.

Sample	ρ [g·cm^{-3}]	atmosphere	Q [kJ.g^{-1}]
PF-1	1.693±0.003	N$_2$	5.8387±0.5665
PF-2	1.693±0.003	N$_2$	6.5657±1.7584
PF-3	1.674±0.003	N$_2$	6.1849±1.8155

lower than that of PF-2, indicating that the reaction priority of Al powder with gaseous detonation products is higher than that of B because of the high melting and boiling points of B_2O_3 coating on the surface of B powder. Firstly, amount of oxygen (O) are assumed during the combustion of Al powder after detonation, leading that there is no enough O to react with B powder. Thus, the calorimetric heat of PF-3 cannot be released completely. Therefore, to achieve high-power explosive under different environments, the mass ratios of Al and B should be specified according to the balance between metallic fuels and oxygen for new metalized explosives.

3.4 Acceleration ability

The process of acceleration of the copper tube by the detonation products was recorded with a high-speed scanning camera. A representative optical film of the copper tube driven by the detonation products of the explosive PF-1 is shown in Figure 5. The experimental detonation velocities of the explosives were also measured during the cylinder expansion test using the copper foil probes method.

The dependence of the external surface radius of the
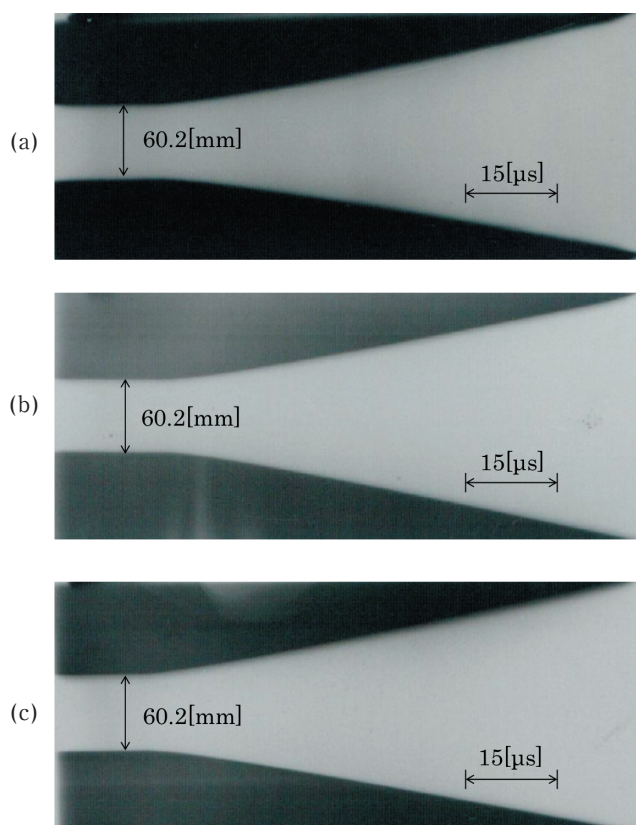
Figure 5   Optical film of the copper tube driven by the detonation products of the explosive (a) PF-1 (b) PF-2 (c) PF-3.

tube on the axial co-ordinate was constructed from the photograph. A large number of experimental data show that the expansion distance and time generated by explosives can be expressed as Equation (1).

$$t = a_1 + a_2 (R - R_0) + a_3 \cdot e^{a_4 (R - R_0)} \tag{1}$$

where t represents the expansion time of cylinder tube wall, μs; a_1, a_2, a_3, a_4 represent the fitting coefficients; R represents the distance between central axis line and outer wall of cylinder, mm: and. R_0 represents the initial distance between central axis line and outer wall of cylinder, mm. Table 5 summarizes the obtained fitting coefficients of cylinder test.

The acceleration ability of an explosive can be described by the so-called Gurney energy E_G, which is defined as a sum of kinetic energies of the driven tube and the detonation products related to unit mass of an explosive. For each expansion state the Gurney energy is calculated by Equation (2).

$$E_G = \frac{U^2}{2} \left(\frac{m}{c} + \frac{1}{2} \right) \tag{2}$$

where, U represents the cylinder wall velocity, mm·μs^{-1}, and m and c represent the metal wall and explosive mass per unit length of cylinder, respectively, kg·mm^{-1}.

The dependence of the tube wall velocity U on the relative volume of the detonation products was determined according to Equation (1). Results are plotted in Figure 6. The tube velocity, determined from the cylinder test results, enables also to estimate the variation of the Gurney energy with the relative volume. The obtained results are presented in Figure 7. These parameters correspond to the tube velocity at the radius where the continuity of tube material is still preserved. Values of the copper tube velocity and Gurney energy at different expansion distances (12 mm, 38 mm, 70 mm) are listed in Table 6.

From Figures 6 and 7, the tube velocity and Gurney energy profiles show that they are similar for all explosives at the very early stage. This is caused by the reaction of the Al contained in the explosive. After about two relative volume of detonation products, the velocities of explosives PF-2 and PF-3 are lower to that obtained for the explosives PF-1, indicating that there is no enough consumed Al and B taking into reaction to push the tube. This is because that the reaction rate of B contained in the explosive is slower than that of Al. The Gurney energy of explosive PF-2 rises up to that of explosive PF-3 at about six relative volume of detonation products, indicating that the amount of consumed B increases with time for explosive PF-2. The combustion heat of B is higher than that of Al, resulting that the explosive PF-2 has a stronger

Table 5   Fitting coefficients of cylinder test.

Sample	a_1	a_2	a_3	a_4
PF-1	5.15452±0.15689	0.72327±0.01963	−4.09039±0.12690	−0.07679±0.00289
PF-2	5.91295±0.17853	0.71559±0.02151	−4.88796±0.14562	−0.06347±0.00365
PF-3	5.44189±0.16561	0.75226±0.02067	−3.92060±0.11596	−0.07443±0.00294
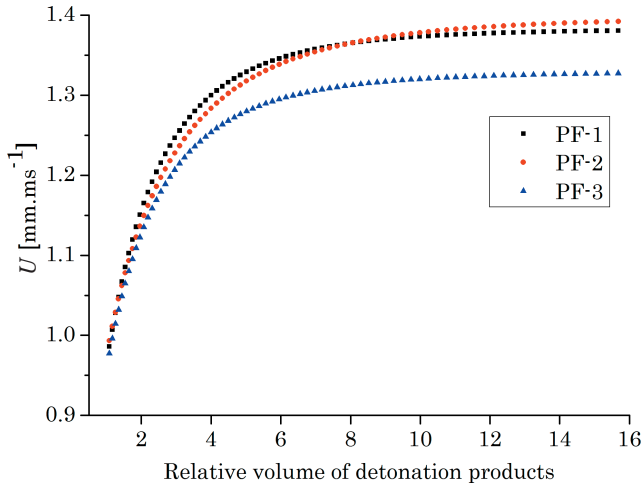
Figure 6   Variation of the copper wall velocity with the relative volume of detonation products.
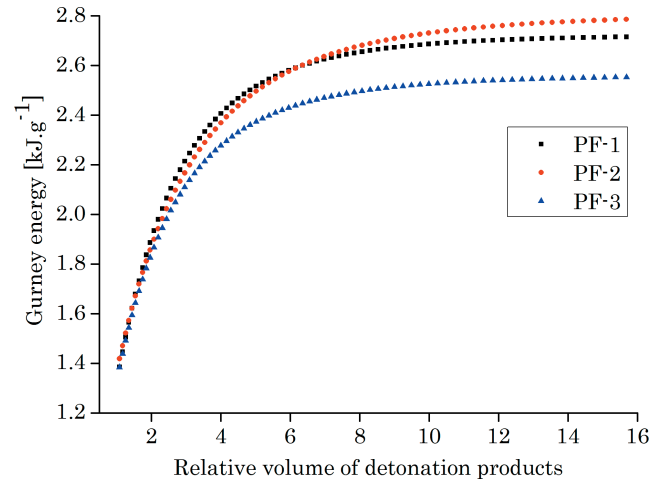
Figure 7   Variation of Gurney energy with the relative volume of detonation products.

Table 6   Copper tube wall velocity and Gurney energy at different expansion distances.

Sample	ρ [g·cm^{-3}]	D [mm·µs^{-1}]	$R-R_0 = 12$ [mm]		$R-R_0 = 38$ [mm]		$R-R_0 = 70$ [mm]	
			U [mm·µs^{-1}]	E_G [kJ·g^{-1}]	U [mm·µs^{-1}]	E_G [kJ·g^{-1}]	U [mm·µs^{-1}]	E_G [kJ·g^{-1}]
PF-1	1.708±0.003	7.812	1.179±0.026	1.980±0.044	1.351±0.028	2.600±0.054	1.380±0.029	2.713±0.057
PF-2	1.689±0.003	7.845	1.162±0.032	1.942±0.049	1.345±0.034	2.602±0.066	1.390±0.035	2.780±0.070
PF-3	1.673±0.003	7.855	1.147±0.029	1.907±0.048	1.300±0.032	2.448±0.060	1.327±0.033	2.550±0.063

afterburning effect ability than that of explosive PF-1. However, considering that there is no enough oxygen to react with B before the disruption of the copper tube for explosive PF-3, the energy of B contained in the explosive cannot be released completely.

Practically, these final values of the tube velocity and Gurney energy before the disruption of the copper tube are important for application in ammunition. Table 6 indicates that they are similar for explosives PF-1 and PF-2 after long expansion distance (70 mm), in which the Gurney energy of explosive PF-2 (2.780 kJ·g^{-1}) is slightly higher than that of explosive PF-1 (2.713 kJ·g^{-1}), and the explosive PF-3 (2.550 kJ·g^{-1}) has the lowest value of Gurney energy. The Gurney energy of explosive PF-3 is lower than that of explosive PF-1 because, as previous results showed, large amount of energy is still available in the detonation products of explosive PF-3 at the relative volume of sixteen.

Comparison of the cylinder test results with the calorimetric explosion heats of the explosives confirms the earlier made conclusion, that a considerable amount of energy was still stored in the detonation products during the relative volume of sixteen permitted by the cylinder test, this is why the Gurney energy of the composites still continued to rise and did not reach a plateau. To a certain extent, the calorimetric bomb tests gave better estimation of the explosion energy. Consequently, it will be judicious in ammunition by adding certain proportion Al and B powder into explosive in which the energy of B can be released easily under the combustion heat of Al and the high pressure of detonation products, in this case the explosion energy of metalized explosive can be maximized.

3.5 JWL isentropes of the detonation products

The most popular equation of state used in hydrocodes is the semi-empirical Jones-Wilkins-Lee (JWL) equation. The JWL equation of the isentrope for the detonation products of condensed explosives has the form as Equation (3).

$$P = A\left(1 - \frac{\omega}{R_1 \overline{V}}\right)e^{-R_1 \overline{V}} + B\left(1 - \frac{\omega}{R_2 \overline{V}}\right)e^{-R_2 \overline{V}} + \frac{\omega E_0}{\overline{V}} \quad (3)$$

where, P represents the pressure of detonation products, GPa; $\overline{V}$ represents the relative specific volume; A and B represent the linear and nonlinear coefficients for a given explosive, respectively, GPa. E_0 represents the initial energy per unit volume of explosives, GPa. Cylinder test data are commonly employed in most methods for the determination of the JWL coefficients.

As determined above, given detonation velocity, detonation pressure, and heat of explosion can be used as input parameters. The relations between the JWL coefficients can be obtained according to the Chapman-Jouguet (CJ) condition and the conservation relation of mass, momentum, and energy.

$$AR_1 e^{-R_1 \overline{V}_J} + BR_2 e^{-R_2 \overline{V}_J} + C\left(\omega + 1\right)\overline{V}_J^{-(\omega + 2)} = \rho_0 D_J^2 \quad (4)$$

$$\frac{A}{R_1}e^{-R_1 \overline{V}_J} + \frac{B}{R_2}e^{-R_2 \overline{V}_J} + \frac{C}{\omega}\overline{V}_J^{-\omega} = E_0 + \frac{1}{2}P_J\left(1 - \overline{V}_J\right) \quad (5)$$

$$Ae^{-R_1 \overline{V}_J} + Be^{-R_2 \overline{V}_J} + C\overline{V}_J^{-(\omega + 1)} = P_J \quad (6)$$

where $\overline{V}_J = k/(k+1), k = \rho_0 D_J^2/P_J - 1$.

Firstly, assuming one set of R_1, R_2, ω according to the JWL coefficients for aluminized explosive with similar formulation, the values of A, B, C can be solved with Equations (4)–(6).
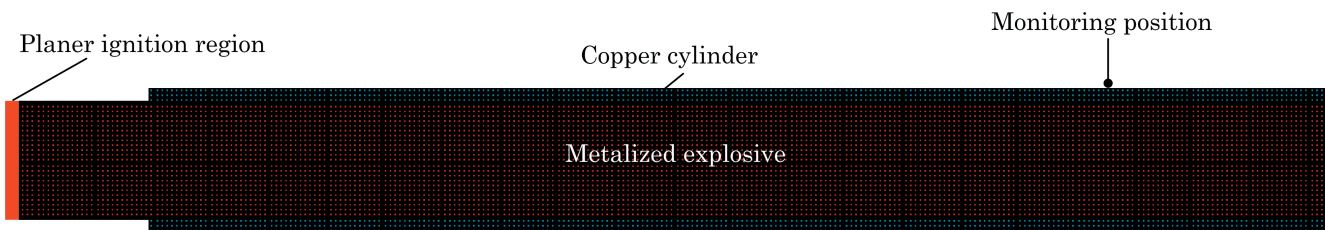
Planer ignition region

Copper cylinder

Monitoring position

Metalized explosive

Figure 8   Computational model of cylinder test.

Table 7   Calculated JWL coefficients.

Explosive	JWL coefficients	
PF-1	$R_1 = 5.22$	$A = 1035.9\,GPa$
	$R_2 = 1.41$	$B = 11.789\,GPa$
	$\omega = 0.26$	$C = 0.93752\,GPa$
	$E_0 = 6.7202\,GPa$	
PF-2	$R_1 = 5.25$	$A = 1150.0\,GPa$
	$R_2 = 1.41$	$B = 8.3522\,GPa$
	$\omega = 0.26$	$C = 1.2125\,GPa$
	$E_0 = 7.2591\,GPa$	
PF-3	$R_1 = 5.12$	$A = 1101.6\,GPa$
	$R_2 = 1.34$	$B = 6.4211\,GPa$
	$\omega = 0.26$	$C = 1.0199\,GPa$
	$E_0 = 6.4632\,GPa$	

Then, a 2D axisymmetric Lagrange cylinder test model has been established according to the real measurement of cylinder test by hydrocode LS-DYNA. The computational model consisting of planer ignition region, metalized explosive, copper cylinder and monitoring position is shown in Figure 8. The metalized explosive is modeled with high explosive burn model and the copper cylinder is modeled with the John-Cook material model and Gruneisen equation of state with the parameters given in literature[24]. The numerical variation curves for wall velocity versus time $v-t$ and expansion radius versus time $(R-R_0)-t$ can be obtained by numerical simulation of explosion driven process.

Comparison of the experimental and numerical variation curves for wall velocity versus time $v-t$ and expansion radius versus time $(R-R_0)-t$, the JWL coefficients for the given explosive are determined until the difference between experimental and numerical values for wall velocity and expansion radius at the same time are less than 1% and 0.5%, respectively. The calculated JWL coefficients are summarized in Table 7. The experimental and numerical isentropes for the explosive PF-2 are presented in Figure 9. The determined JWL isentropes and equations of state for the detonation products of the novel metalized explosives can be used for modeling and simulation of the processes accompanying the detonation of charges made from these explosives.

4. Conclusions

This study reports a new orientation for the design of industrial explosive and military explosive such as (HMX/Al/B) system.

We have found that the advantages of boron (high heating value) and aluminum (reacted earlier and high
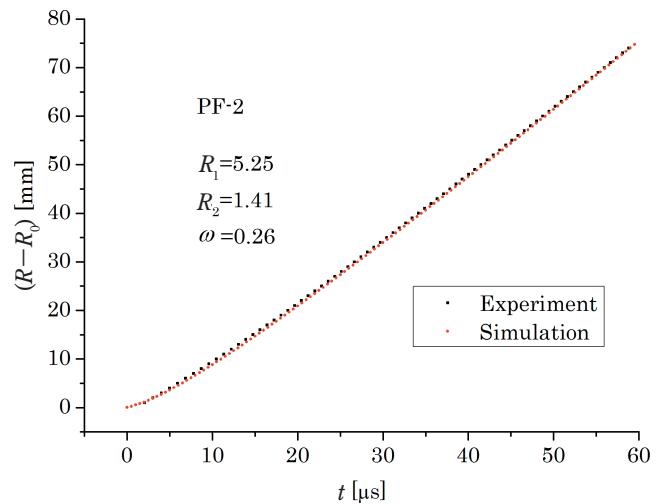
Figure 9   Experimental and numerical isentropes for the explosive PF-2.

burning temperature) powder can be largely utilized when two kinds of metal powders are mixed in a certain proportion. The energetic characteristics of metalized explosives containing B/Al, such as heat of explosion and acceleration ability, show obvious advantage than explosive containing pure aluminum, but not for the detonation pressure and detonation velocity. Thus the B/Al compound powder is chemically inert in the detonation reaction zone, and the energy of B can be released easily under the combustion heat of Al after detonation, called the combination effect.

We also found that when the content of B exceeds a critical value, it shows a downward trend both in heat of explosion and acceleration ability, indicating that the mass ratio of Al and B should be specified according to their different action in the reaction. Therefore, there need a further work to identify the optimum formulation by refining the content and proportion of Al and B.

Acknowledgements

References

1) N. H. Yen and L. Y. Wang, Propellants, Explos., Pyrotech., 37, 143−155 (2012).
2) N. S. Cohen, AIAA J., 7, 1345−1352 (1969).
3) M. D. Clemenson, S. Johnson, H. Krier, and N. Glumac, Propellants, Explos., Pyrotech., 39, 454−462 (2014).
4) M. A. Cook, A. S. Filler, R. T. Keyes, W. S. Partridge, and W. Ursenbach, J. Phys. Chem., 61, 189−196 (1957).

5) M. N. Makhov, M. F. Gogulya, A. Y. Dolgoborodov, M. A. Brazhnikov, V. I. Arkhipov, and V. I. Pepekin, Combust. Explos. Shock Waves, 40, 458−466 (2004).

6) E. L. Baker, C. Capellos, and L. I. Stiel, Sci. Tech. Energetic Materials, 67, 134−138 (2006).

7) I. M. Shyu and T. K. Liu, Combust. Flame, 100, 634−644 (1995).

8) J. R. Luman, B. Wehrman, K. K. Kuo, R. A. Yetter, N. M. Masoud, T. G. Manning, L. E. Harris, and H. A. Bruck, Proc. Combust. Inst., 31, 2089−2096 (2007).

9) W. Jung, S. Baek, J. Park, and S. Kwon, J. Propul. Power, 34, 1070−1079 (2018).

10) C. L. Yeh and K. K. Kuo, Prog. Energ. Combust. Sci., 22, 511 −541 (1996).

11) J. G. Speight, "Lange's Handbook of Chemistry", McGraw-Hill (2005).

12) M. D. Clemenson, S. Johnson, H. Krier, and N. Glumac, Propellants, Explos., Pyrotech., 39, 454−462 (2014).

13) K. P. Brooks and M. W. Beckstead, J. Propuls. Power, 11, 769 −780 (2012).

14) X. S. Feng, S. X. Zhao, X. Q. Diao, and Z. X. Dai, Chin. J. Explos. Propellants, 32, 21−24 (2009). (in Chinese).

15) E. L. Baker, D. Murphy, D. Suarez, C. Capellos, P. Cook, P. Anderson, E. Wrobel, and L. Stiel, U.S. Army Technical Report ARMET−TR−10004, Picatinny Arsenal (2010).

16) M. N. Makhov, Russ. J. Phys. Chem. B, 9, 50−55 (2015).

17) K. Lee and J. Kim, Proc. 36th Annual Conference (International) of ICT, Karlsruhe, Germany (2005).

18) S. Xu, Y. Chen, X. Chen, D.Wu, and D. Liu, Combust. Explos. Shock Waves, 52, 342−349 (2016).

19) Y. Chen, S. Xu, D. J. Wu and D. B. Liu, Cent. Eur. J. Energ. Mater., 13, 117−134 (2016).

20) National Military Standard of China, GJB772A−1997 (1997).

21) D. Frem, Z. Anorg. Allg. Chem., 10.1002/zaac.201700395 (2017).

22) W. Kicinski and W. A. Trzcinski, J. Therm. Anal. Calorim., 96, 623−630 (2009).

23) D. L. Ornellas, "Calorimetric determinations of the heat and products of detonation for explosives: October 1961 to April 1982," Lawrence Livermore National Laboratory Report UCRL−52821, Lawrence Livermore (1982).

24) L. Maiz, W. A. Trzcinski, M. Szala, J. Paszula, and K. Karczewski, Cent. Eur. J. Energ. Mater., 13, 957−977 (2016).